Redox-Non-Innocent Ligands

DOI: 10.1002/ange.201309948

The Formazanate Ligand as an Electron Reservoir: Bis(Formazanate) Zinc Complexes Isolated in Three Redox States**

*Mu-Chieh Chang, Thomas Dann, David P. Day, Martin Lutz, Gregory G. Wildgoose, and Edwin Otten**

Abstract: *The synthesis of bis(formazanate) zinc complexes is described. These complexes have well-behaved redox-chemistry, with the ligands functioning as a reversible electron reservoir. This allows the synthesis of bis(formazanate) zinc compounds in three redox states in which the formazanate ligands are reduced to "metallaverdazyl" radicals. The stability of these ligand-based radicals is a result of the delocalization of the unpaired electron over four nitrogen atoms in the ligand backbone. The neutral, anionic, and dianionic compounds ($L_2Zn^{0/-1/-2}$) were fully characterized by single-crystal X-ray crystallography, spectroscopic methods, and DFT calculations. In these complexes, the structural features of the formazanate ligands are very similar to well-known β-diketiminates, but the nitrogen-rich (NNCNN) backbone of formazanates opens the door to redox-chemistry that is otherwise not easily accessible.*

Metal-mediated redox processes are of fundamental importance in a wide variety of bond formation and cleavage reactions. The utility of transition-metal catalysts in this type of reactions stems from their ability to switch between two (or more) oxidation states. Recently, there has been increased interest in redox processes that do not occur at the metal center, but instead take place within the ancillary ligand framework (so-called "redox-active" or "non-innocent" ligands).[1] The use of organic ligands as redox equivalents is of key importance in biological (enzymatic) transformations,[2] and has been shown to open new reactivity pathways in catalysis.[1c] The most studied ligands of this class are dithiolenes and dioxolenes, while recent work has focused on α-diimines[3] and bis(imino)pyridines.[4]

A class of ligands that has found widespread utility in the synthesis of metal complexes across the periodic table are the monoanionic β-diketiminates.[5] These are generally considered as stable ligand scaffolds without involvement in redox chemistry. Recently, examples of β-diketiminate metal complexes were reported in which the ligand was either reduced to a metal-bound di- or trianion,[6] or oxidized to a neutral radical species.[7] However, the limited stability of β-diketiminate complexes upon changing oxidation state prevents widespread application.[8]

Formazanates (1,2,4,5-tetraazapentadienyls),[9] which are close analogues of β-diketiminates, have received comparatively little attention as ligands in coordination chemistry.[10] The stability of organic six-membered heterocyclic radicals (verdazyls) that are derived from formazans prompted us to explore the use of formazanates as potential redox-active ligands. Herein we show that zinc complexes with formazanate ligands engage in remarkably facile and reversible redox chemistry that allows the full characterization of bis(formazanate) L_2Zn complexes in charge neutral, anionic or dianionic redox states.

Bis(formazanate) zinc complexes are readily accessible by protonolysis of Me_2Zn with the neutral ligand precursors PhNNC(*p*-tol)NNHPh (**1a**) and PhNNCH(*t*Bu)NNPh (**1b**). In the case of formazan **1a**, an immediate color change from red to intense blue is observed to indicate formation of the bis(formazanate) complex [(PhNNC(*p*-tol)NNPh)$_2$Zn] (**2a**, Scheme 1). Yellow **1b** also reacts immediately with Me_2Zn, but in this case heating to 50 °C overnight was required to obtain full conversion to [(PhNNC(*t*Bu)NNPh)$_2$Zn] (**2b**,

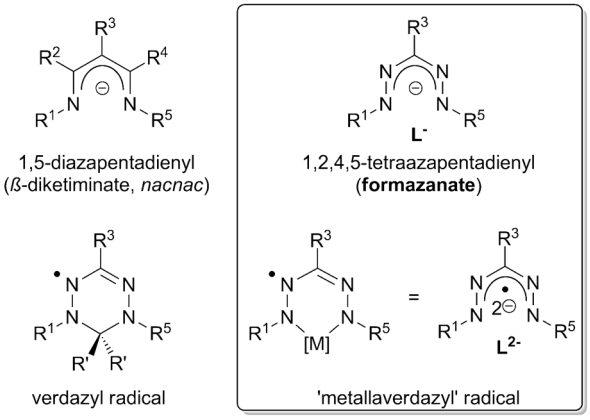

[*] M.-C. Chang, Dr. E. Otten
Stratingh Institute for Chemistry, University of Groningen
Nijenborgh 4, 9747 AG Groningen (The Netherlands)
E-mail: edwin.otten@rug.nl
Dr. M. Lutz
Bijvoet Center for Biomolecular Research
Crystal and Structural Chemistry, Utrecht University
Padualaan 8, 3584 CH Utrecht (The Netherlands)
T. Dann, Dr. D. P. Day, Dr. G. G. Wildgoose
Energy & Materials Laboratory, School of Chemistry
University of East Anglia
Norwich Research Park, Norwich, NR4 7TJ (UK)

[**] G.G.W. and D.P.D. thank the European Research Council for funding (ERC Grant Agreement no. ERC-StG-307061 PiHOMER). G.G.W. thanks the Royal Society for additional support via a University Research Fellowship. T.D. thanks the University of East Anglia for financial support via a Dean's studentship. NWO is gratefully acknowledged for funding (Veni grant to E.O.). We thank Prof. B. de Bruin (University of Amsterdam) for help with VT-EPR experiments and A. Meetsma for useful discussions on the X-ray crystallography.

Supporting information for this article is available on the WWW under http://dx.doi.org/10.1002/anie.201309948.

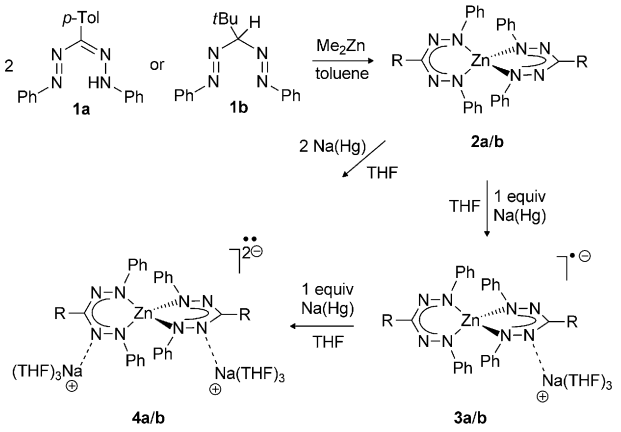

Scheme 1. Synthesis of neutral, monoanionic, and dianionic bis(formazanate)zinc complexes.

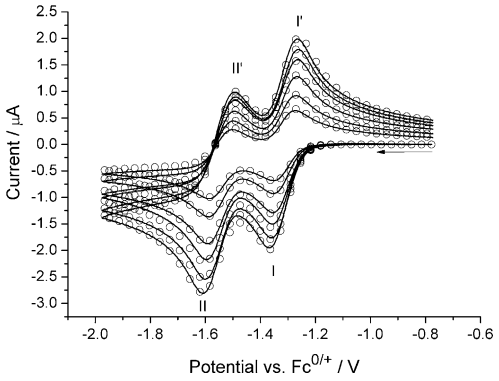

Figure 2. Cyclic voltammograms of a 2.5 mM solution of **2a** in THF (0.1 M $[Bu_4N][B(C_6F_5)_4]$) recorded at 100, 200, 400, 600, 800, and 1000 $mV s^{-1}$. Solid lines are experimental data; open circles are simulated data.

Scheme 1). Both complexes are obtained in good yield (>75%) by crystallization as intensely colored solids. Single-crystal X-ray diffraction studies (Figure 1; Supporting Information, Figure S1; pertinent bond distances in Table 2 and Supporting Information, Table S2) reveal a very similar tetrahedral geometry around the central Zn atom.[11] As is the case in related β-diketiminate complexes, full delocalization within the formazanates is indicated by the equivalent N–N and C–N bond lengths in the backbone of each ligand.[12]

To establish the redox-active nature of the formazanate ligands in compounds **2**, we ran cyclic voltammetry experiments in THF solution with $[Bu_4N][B(C_6F_5)_4]$ electrolyte.[13] Upon scanning in a reductive direction the CV shows two quasi-reversible, single-electron redox processes, labeled system I/I′ and II/II′ (Figure 2). These correspond to the reversible formation of the radical anions of **2a** and **2b** ($\mathbf{2a}^{\bullet-}$ or $\mathbf{2b}^{\bullet-}$; system I/I′) and the corresponding dianions ($\mathbf{2a}^{2-}$ or $\mathbf{2b}^{2-}$; system II/II′), respectively. If the scan direction is reversed after the reductive peak I but before peak II, then the reoxidation of the radical anion ($\mathbf{2a}^{\bullet-}$ or $\mathbf{2b}^{\bullet-}$) is once again observed as peak I′, indicating that each redox process is sequential and independent. When the scan rate is varied between 100 and 1000 $mV s^{-1}$, all processes exhibited a linear relationship between peak current and the square root of the voltage scan rate, which is indicative of diffusion-controlled redox processes. Excellent fits between experiment and digital simulation of the cyclic voltammetry of **2a** and **2b** (Figure 2) yielded optimized values of formal potentials E^0 and electron transfer rate constants k^0 listed in Table 1.

Table 1: Optimized electron transfer parameters determined from digital simulation of experimental voltammetry.

	E^0 vs $Fc^{0/+}$ [V]	k^0 [10^{-2} cm s^{-1}]
2a		
system I/I′	−1.31 ± 0.01	1.25 ± 0.05
system II/II′	−1.55 ± 0.01	0.90 ± 0.05
2b		
system I/I′	−1.57 ± 0.01	1.30 ± 0.05
system II/II′	−1.85 ± 0.02	0.75 ± 0.05

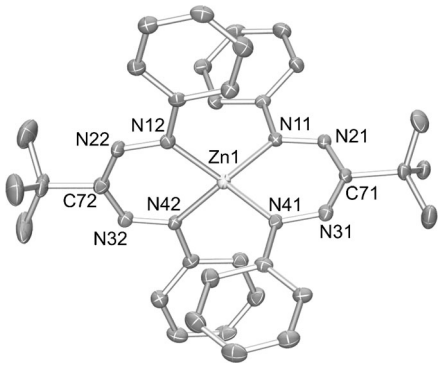

Figure 1. Molecular structure of **2b**. Ellipsoids set at 50%; hydrogen atoms are omitted for clarity.

Replacing the inductively electron-donating *tert*-butyl group with the electron withdrawing *p*-tolyl group on the formazanate ligands has the expected effect on the reduction potentials (Table 1). Interestingly, the one-electron reduction of both bis(formazanate)zinc complexes **2a** and **2b** occurs at more negative potentials ($E^0_{I/I'} = -1.31$ V vs. $Fc^{0/+}$, **2a**; −1.57 V vs. $Fc^{0/+}$, **2b**) than Hicks and co-workers have reported for boron mono(formazanate) compounds ($E^0 \approx -0.9$ V vs. Fc/Fc^+).[14] This likely reflects the different Lewis acidity of the boron and zinc centers together with a different degree of covalency in the metal–ligand bonding. Cyclic voltammetric characterization indicates that both the singly reduced radical anion and the doubly reduced dianionic states of **2a** and **2b** are synthetically accessible.

In accordance with the CV data, the chemical reduction of neutral bis(formazanate) complexes **2a** and **2b** could be accomplished by treatment with 1.0 equiv of Na(Hg) in THF. The resulting radical species $[Na(THF)_3][(PhNNC(R)NNPh)_2Zn]$ (R = *p*-tolyl, **3a**; R = *t*Bu, **3b**) could be isolated as crystalline material by slow diffusion of hexane into the THF solution (Scheme 1). Compounds **3a** and **3b** are NMR-silent but show broad EPR signals (*g*-value ≈2) both in THF and the solid state (298 and 77 K) that are

devoid of observable hyperfine coupling (Supporting Information, Figure S3).

The crystallographically determined structures (Figure 3; Supporting Information, Figure S1; pertinent bond distances in Table 2 and Table S2) show that the tetrahedral L_2Zn^- radical anion interacts with a $Na(THF)_3^+$ cation through one (**3a**) or two (**3b**) nitrogen atoms of a formazanate ligand.[11] A closer inspection of the metrical parameters within the formazanate backbone reveals that there are two distinctly different ligands in the L_2Zn^- fragment. One of the formazanates is very similar to those in the neutral precursors **2** (av. Zn-N: 2.014 Å; N-N: 1.304 Å), while the formazanate that binds the $Na(THF)_3^+$ has shortened Zn–N (av. 1.957 Å) and elongated N–N bonds (av. 1.363 Å). Thus, the L_2Zn^- anion is best described as a Zn^{2+} center coordinated by a "normal" monoanionic formazanate (L^-) and a reduced dianionic ligand (L^{2-}). The Zn-coordinated L^{2-} fragment can be considered an inorganic analogue of a verdazyl radical.[15] The long N–N bonds in the L^{2-} fragment result from the unpaired electron occupying a molecular orbital (SOMO), which has π* N–N anti-bonding character (see below). The observation of two distinct ligand redox states is likely related to electrostatic interactions with the cation, which localizes the additional negative charge. A similar situation is observed in related bis(ligand) complexes: in the case of neutral radical species $[\{PhB(\mu\text{-}NtBu)_2\}_2M]$ (M = Al, Ga)[16] and [(β-diketiminate)$_2$Al],[17] the unpaired electron is fully delocalized over the spirocyclic structure, while for the radical anions $[\{PhB(\mu\text{-}NtBu)_2\}_2M^-]$ (M = Mg, Zn), localized spin density is observed owing to interaction with the cation.[18]

As suggested by the CV measurements, compounds **3** react with an additional equivalent of Na amalgam to give the dianionic complexes $[Na(THF)_3]_2[(PhNNC(R)NNPh)_2Zn]$ (R = *p*-tolyl, **4a**; R = *t*Bu, **4b**), of which **4b** was crystallographically characterized (Figure 4; pertinent bond distances in Table 2).[11] It contains two sodium cations that both interact with two N atoms of a different formazanate ligand. The presence of an additional electron in both ligands (L^{2-}) is evidenced by the similar bond lengths in **4b**, which are elongated in comparison to the neutral precursor **2b** (Table 2).

Table 2: Selected bond distances in **2b**, **3b**, and **4b**.

	2b	**3b**	**4b**
Zn1–N11	1.9824(17)	1.9857(16)	1.9793(14)
Zn1–N41	1.9822(18)	2.0207(16)	1.9839(14)
Zn1–N12	1.9902(17)	1.9447(16)	1.9696(14)
Zn1–N42	1.9769(18)	1.9657(16)	1.9952(15)
N11–N21	1.310(2)	1.313(2)	1.359(2)
N31–N41	1.307(2)	1.295(2)	1.376(2)
N12–N22	1.307(2)	1.360(2)	1.355(2)
N32–N42	1.309(2)	1.370(2)	1.378(2)

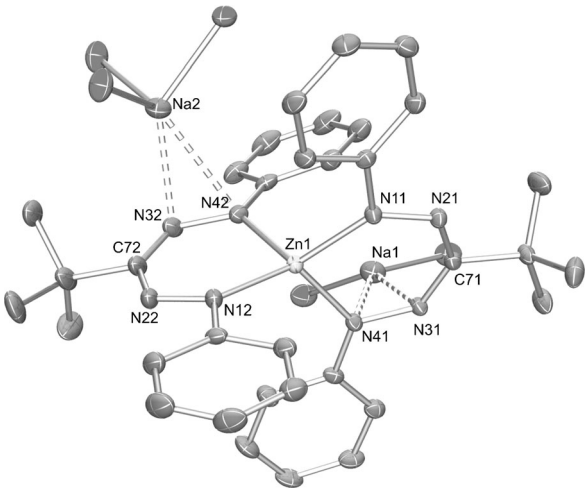

Figure 4. Molecular structure of **4b**. Ellipsoids set at 50%; hydrogen atoms and also carbon atoms of the THF moieties are omitted for clarity.

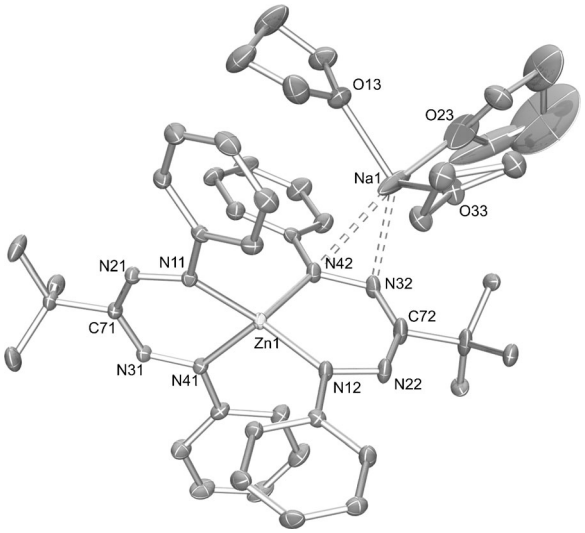

Figure 3. Molecular structure of **3b**. Ellipsoids set at 50%; hydrogen atoms are omitted for clarity.

EPR spectra of diradicals[19] **4a** and **4b** in frozen THF solution (77 K) are very similar and show features indicative of randomly oriented triplets ($g = 2.0028$) with characteristic half-field ($\Delta m_s = 2$) signals (Figure 5). The zero-field splitting

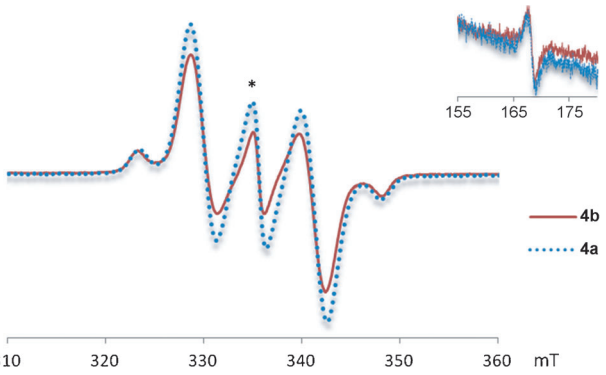

Figure 5. EPR spectra (frozen THF solution) of **4a** and **4b** (asterisk denotes a doublet impurity). Inset: half-field region.

parameters $D = 11.6 \times 10^{-3}$ and $11.5 \times 10^{-3}\,cm^{-1}$ from the EPR spectra for **4a** and **4b**, respectively, are somewhat smaller than those in the neutral triplet diazabutadiene complex [(tBu$_2$DAB)$_2$Zn] ($23.1 \times 10^{-3}\,cm^{-1}$),[20] and comparable to D-values found for purely organic phenylene-linked bis(radical) compounds (radical = semiquinone;[21] verdazyl),[22] which range between about $4–10 \times 10^{-3}\,cm^{-1}$. It should be noted that although metal complexes with coordinated verdazyl radicals have been prepared,[23] compounds **4** are the first examples of diradical "metallaverdazyl" compounds.

UV/Vis spectroscopy of neutral, anionic, and dianionic bis(formazanate) zinc compounds (Supporting Information, Figure S2) provides additional evidence for ligand-based reduction and formation of verdazyl-type (L^{2-}) ligands. The neutral compounds **2a** and **2b** show single broad absorptions in the visible range at 578 and 536 nm, respectively. The singly reduced compounds **3** have both formazanate (L^{-}) and one-electron reduced, verdazyl-type (L^{2-}) ligands. As a consequence, they feature new absorption bands at longer (**3a**/**3b**: 769/755 nm) and shorter wavelengths (**3a**/**3b**: 508/462 nm) owing to L^{2-}; the position of these bands is similar to that observed in organic (Kuhn-type) triarylverdazyls.[24] Furthermore, a weakened and bathochromically shifted absorption is observed, which is attributed to the L^{-} fragment in **3a**/**b**. For compounds **4a** and **4b**, the intensity of the low and high energy absorptions due to the L^{2-} fragment is increased relative to the singly reduced species **3**. The most prominent absorptions in the visible range are at 510/798 (**4a**) and 436/755 nm (**4b**), in agreement with the presence of only reduced formazanate (verdazyl-type) ligands.

DFT calculations were carried out to examine the electronic structure of the complexes described herein. The crystallographically determined bond lengths and angles are reproduced accurately by (unrestricted) B3LYP/6-31G(d) calculations using Gaussian 09 starting from the X-ray coordinates. However, geometry optimization of the "free" radical anions **3** at the UB3LYP/6-31G(d) level of theory resulted in structures in which the SOMO is delocalized over both ligands. For example, in **3a**$_{calc}$ the diagnostic N–N bond lengths are all equivalent at about 1.322 Å, in between the short (L^{-}: av. 1.304 Å) and long N–N bonds (L^{2-}: av. 1.361 Å) observed experimentally. When the countercation [Na(THF)$_3$]$^+$ that is present in the crystal structure determination is included in the computations, the unpaired electron is localized (see Figure 6 for **3a**$_{calc}$). This is in agreement with the experimental data and suggests that electrostatic effects are responsible for this localization. The calculated hyperfine interactions with the ^{14}N nuclei are small in **3a**$_{calc}$ (< 2.1 G), which likely accounts for the broad, featureless EPR signals observed experimentally.

For the diradicals **4**, geometry optimizations of the L_2Zn^{-2} fragment in the absence of countercations converges at structures that have two (virtually) identical L^{-2} ligands with elongated N–N bond lengths of about 1.346 Å, which is somewhat shorter than those observed experimentally for **4b** (av. 1.367 Å). Broken-symmetry DFT calculations[25] show two ligand-based unpaired electron spins that are antiferromagnetically coupled ($J_{calcd} = -7.9\,cm^{-1}$) to give a singlet diradical ground state (Figure 6). The calculated spin density in diradical **4a**$_{calc}$ indicates that the unpaired electrons are located at the nitrogen atoms of the ligands, with some contribution of the aromatic substituents. To verify experimentally the ground state of **4a**, preliminary EPR studies were carried out in the temperature range of 6–60 K (THF glass) to determine the temperature dependence of the EPR signal intensity I. A plot of $I \times T$ vs. T shows that $I \times T$ decreases upon lowering the temperature (Supporting Information, Figure S4). This behavior is indicative of a singlet diradical ground state,[19] thus corroborating our computational results. Although singlet biradical species like **4** are rare, Roesky and co-workers recently reported a dicarbene zinc compound for which the singlet diradical was calculated to be lower in energy than the triplet by about 4 kcal mol^{-1}.[26]

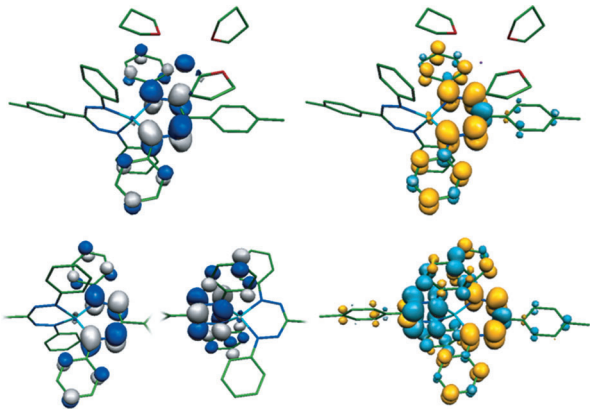

Figure 6. Top: SOMO (left) and spin density plot (right) for **3a**$_{calc}$. Bottom: Two ligand-centered SOMOs for the BS(1,1) solution (truncated structures, left) and spin density plot (right) for **4a**$_{calc}$.

In conclusion, we have shown that complexes with formazanate ligands give rise to reactivity that is not accessible with their β-diketiminate congeners. Bis(formazanate) zinc complexes engage in remarkably facile reductive chemistry to give isolable one- and two-electron reduction products of L_2Zn, the stability of which results from the "metallaverdazyl"-type structures obtained. The use of coordinated formazanates as reversible electron reservoir in (catalytic) reactions is currently under investigation in our laboratory.

Experimental Section

[(PhNNC(p-tolyl)NNPh)$_2$Zn] (**2a**): A 1.2 M solution of Me$_2$Zn in toluene (0.82 mL, 0.98 mmol) was added slowly to a suspension of PhNNC(p-tolyl)NNHPh (620 mg, 1.97 mmol) in toluene (10 mL) at room temperature. The mixture was stirred for 2 h after which the color had changed to intense blue. The volatiles were removed in vacuo and the residue was subsequently extracted into a hot 3:1 hexane/toluene mixture. Slow cooling of the clear dark blue solution to −30 °C for 2 days afforded 552 mg dark violet crystals of [(PhNNC(p-tolyl)NNPh)$_2$Zn]·(toluene)$_{0.5}$ (0.75 mmol, 76 %). ^{1}H NMR (200 MHz, C$_6$D$_6$, 25 °C): $\delta = 8.42$ (d, 2H, $J = 7.9$, p-tolyl CH), 7.70 (d, 4H, $J = 7.8$, Ph o-H), 7.29 (d, 2H, $J = 7.9$, p-tolyl CH), 6.81 (t, 4H, $J = 7.7$, Ph m-H), 6.66 (t, 2H, $J = 7.4$, Ph p-H), 2.25 ppm (s, 3H, p-tolyl CH$_3$). ^{13}C NMR (50.4 MHz, C$_6$D$_6$, 25 °C): $\delta = 152.8$ (Ph $ipso$-C), 144.0

(NCN), 137.6 (*p*-tolyl *ipso*-C), 137.1 (*p*-tolyl *C*Me), 129.7 (Ph *m*-CH), 129.6 (*p*-tolyl CH), ca. 127.5 (overlapped, Ph *p*-CH), 126.4 (*p*-tolyl CH), 120.2 (Ph *o*-CH), 21.2 ppm (*p*-tolyl CH_3). Anal. calcd for $C_{43.5}H_{38}N_8Zn$: C 70.78, H 5.19, N 15.18; found: C 70.74, H 5.21, N 15.13.

$[Na(THF)_3]^+[(PhNNC(p\text{-tolyl})NNPh)_2Zn]^-$ (**3a**): One leg of a double-Schlenk flask was charged with **2a** (750 mg, 1.02 mmol), Na(Hg) (2.447 wt % Na; 1222 mg, 1.30 mmol), and THF (15 mL). The reaction mixture was stirred for overnight, filtered, and reduced to half of the original volume. Slow diffusion of hexane (15 mL) into the THF solution precipitated 658 mg of $[Na(THF)_3]^+[(PhNNC(p\text{-tolyl})NNPh)_2Zn]^-$ as brown crystalline material (0.707 mmol, 69 %). Anal. calcd for $C_{52}H_{58}N_8NaO_3Zn$: C 67.05, H 6.28, N 12.03; found: C 66.84, H 6.25, N 11.90.

$[Na(THF)_3]^+_2[(PhNNC(p\text{-tolyl})NNPh)_2Zn]^{2-}$ (**4a**): A mixture of solid **2a** (50 mg, 0.068 mmol) and Na/Hg (149.5 mg; 2.447 wt % Na; 3.7 mg Na, 0.159 mmol) was prepared. THF (7 mL) was added with stirring at room temperature. After stirring the reaction mixture one week, pentane (28 mL) was added at room temperature to precipitate the product. The supernatant was decanted and the crystalline product washed with pentane to give $[Na(THF)_3]^+_2[(PhNNC(p\text{-tolyl})NNPh)_2Zn]^{2-}$ as green crystalline material (30.0 mg; 0.026 mmol, 39 %). Anal. calcd for $C_{64}H_{82}N_8Na_2O_6Zn$: C 65.55, H 7.06, N 9.57; found: C 65.53, H 6.89, N 9.87.

Received: November 15, 2013
Revised: January 22, 2014
Published online: February 24, 2014

Keywords: formazanate · N ligands · radical ligands · redox chemistry · zinc

[1] a) P. J. Chirik, K. Wieghardt, *Science* **2010**, *327*, 794; b) W. I. Dzik, J. I. van der Vlugt, J. N. H. Reek, B. de Bruin, *Angew. Chem.* **2011**, *123*, 3416; *Angew. Chem. Int. Ed.* **2011**, *50*, 3356; c) V. Lyaskovskyy, B. de Bruin, *ACS Catal.* **2012**, *2*, 270.
[2] L. Que, W. B. Tolman, *Nature* **2008**, *455*, 333.
[3] H. Tsurugi, T. Saito, H. Tanahashi, J. Arnold, K. Mashima, *J. Am. Chem. Soc.* **2011**, *133*, 18673.
[4] a) M. W. Bouwkamp, A. C. Bowman, E. Lobkovsky, P. J. Chirik, *J. Am. Chem. Soc.* **2006**, *128*, 13340; b) S. C. Bart, K. Chlopek, E. Bill, M. W. Bouwkamp, E. Lobkovsky, F. Neese, K. Wieghardt, P. J. Chirik, *J. Am. Chem. Soc.* **2006**, *128*, 13901; c) J. M. Darmon, S. C. E. Stieber, K. T. Sylvester, I. Fernández, E. Lobkovsky, S. P. Semproni, E. Bill, K. Wieghardt, S. DeBeer, P. J. Chirik, *J. Am. Chem. Soc.* **2012**, *134*, 17125; d) A. M. Tondreau, S. C. E. Stieber, C. Milsmann, E. Lobkovsky, T. Weyhermüller, S. P. Semproni, P. J. Chirik, *Inorg. Chem.* **2013**, *52*, 635.
[5] L. Bourget-Merle, M. F. Lappert, J. R. Severn, *Chem. Rev.* **2002**, *102*, 3031.
[6] a) A. G. Avent, P. B. Hitchcock, A. V. Khvostov, M. F. Lappert, A. V. Protchenko, *Dalton Trans.* **2004**, 2272; b) O. Eisenstein, P. B. Hitchcock, A. V. Khvostov, M. F. Lappert, L. Maron, L. Perrin, A. V. Protchenko, *J. Am. Chem. Soc.* **2003**, *125*, 10790; c) A. G. Avent, A. V. Khvostov, P. B. Hitchcock, M. F. Lappert, *Chem. Commun.* **2002**, 1410.
[7] M. M. Khusniyarov, E. Bill, T. Weyhermüller, E. Bothe, K. Wieghardt, *Angew. Chem.* **2011**, *123*, 1690; *Angew. Chem. Int. Ed.* **2011**, *50*, 1652.
[8] a) F. Basuli, U. J. Kilgore, D. Brown, J. C. Huffman, D. J. Mindiola, *Organometallics* **2004**, *23*, 6166; b) H. Hamaki, N. Takeda, N. Tokitoh, *Organometallics* **2006**, *25*, 2457; c) G. Bai, P. Wei, D. W. Stephan, *Organometallics* **2006**, *25*, 2649; d) N. C. Tomson, J. Arnold, R. G. Bergman, *Organometallics* **2010**, *29*, 5010.
[9] A. W. Nineham, *Chem. Rev.* **1955**, *55*, 355.
[10] a) J. B. Gilroy, B. O. Patrick, R. McDonald, R. G. Hicks, *Inorg. Chem.* **2008**, *47*, 1287; b) J. B. Gilroy, M. J. Ferguson, R. McDonald, R. G. Hicks, *Inorg. Chim. Acta* **2008**, *361*, 3388; c) S. Hong, L. M. R. Hill, A. K. Gupta, B. D. Naab, J. B. Gilroy, R. G. Hicks, C. J. Cramer, W. B. Tolman, *Inorg. Chem.* **2009**, *48*, 4514.
[11] CCDC 972163, 972164, 972165, 972166, and 972167 contain the supplementary crystallographic data for this paper. These data can be obtained free of charge from The Cambridge Crystallographic Data Centre via www.ccdc.cam.ac.uk/data_request/cif.
[12] a) M. Cheng, D. R. Moore, J. J. Reczek, B. M. Chamberlain, E. B. Lobkovsky, G. W. Coates, *J. Am. Chem. Soc.* **2001**, *123*, 8738; b) Y.-C. Tsai, *Coord. Chem. Rev.* **2012**, *256*, 722.
[13] W. E. Geiger, F. Barrière, *Acc. Chem. Res.* **2010**, *43*, 1030.
[14] J. B. Gilroy, M. J. Ferguson, R. McDonald, B. O. Patrick, R. G. Hicks, *Chem. Commun.* **2007**, 126.
[15] "Verdazyls and Related Radicals Containing the Hydrazyl [R_2N-NR] Group": R. G. Hicks in *Stable Radicals*, Wiley, Hoboken, **2010**, p. 245.
[16] T. Chivers, D. J. Eisler, C. Fedorchuk, G. Schatte, H. M. Tuononen, R. T. Boere, *Chem. Commun.* **2005**, 3930.
[17] J. Moilanen, J. Borau-Garcia, R. Roesler, H. M. Tuononen, *Chem. Commun.* **2012**, *48*, 8949.
[18] T. Chivers, D. J. Eisler, C. Fedorchuk, G. Schatte, H. M. Tuononen, R. T. Boeré, *Inorg. Chem.* **2006**, *45*, 2119.
[19] M. Abe, *Chem. Rev.* **2013**, *113*, 7011.
[20] M. G. Gardiner, G. R. Hanson, M. J. Henderson, F. C. Lee, C. L. Raston, *Inorg. Chem.* **1994**, *33*, 2456.
[21] a) D. A. Shultz, A. K. Boal, D. J. Driscoll, J. R. Kitchin, G. N. Tew, *J. Org. Chem.* **1995**, *60*, 3578; b) D. A. Shultz, A. K. Boal, G. T. Farmer, *J. Org. Chem.* **1998**, *63*, 9462.
[22] a) R. M. Fico, M. F. Hay, S. Reese, S. Hammond, E. Lambert, M. A. Fox, *J. Org. Chem.* **1999**, *64*, 9386; b) J. B. Gilroy, S. D. J. McKinnon, P. Kennepohl, M. S. Zsombor, M. J. Ferguson, L. K. Thompson, R. G. Hicks, *J. Org. Chem.* **2007**, *72*, 8062.
[23] a) T. M. Barclay, R. G. Hicks, M. T. Lemaire, L. K. Thompson, *Inorg. Chem.* **2001**, *40*, 6521; b) D. J. R. Brook, G. T. Yee, M. Hundley, D. Rogow, J. Wong, K. Van-Tu, *Inorg. Chem.* **2010**, *49*, 8573; c) K. J. Anderson, J. B. Gilroy, B. O. Patrick, R. McDonald, M. J. Ferguson, R. G. Hicks, *Inorg. Chim. Acta* **2011**, *374*, 480.
[24] R. Kuhn, H. Trischmann, *Monatsh. Chem.* **1964**, *95*, 457.
[25] F. Neese, *Coord. Chem. Rev.* **2009**, *253*, 526.
[26] A. P. Singh, P. P. Samuel, H. W. Roesky, M. C. Schwarzer, G. Frenking, N. S. Sidhu, B. Dittrich, *J. Am. Chem. Soc.* **2013**, *135*, 7324.

